

Quantum Simulation of Nuclear Inelastic Scattering

January 29, 2022

Weijie Du^{a,b,c,*}, James P. Vary^a, Xingbo Zhao^{b,c}, and Wei Zuo^{b,c}

^a*Department of Physics and Astronomy, Iowa State University, Ames, Iowa 50010, USA*

^b*Institute of Modern Physics, Chinese Academy of Sciences, Lanzhou 730000, China*

^c*School of Nuclear Science and Technology, University of Chinese Academy of Sciences, Beijing 100049, China*

Abstract

We present the hybrid quantum/classical algorithm for nuclear inelastic scattering in the time-dependent basis function on qubits approach. It is a non-perturbative approach for simulating these processes on quantum computers. Working in the interaction picture and dividing the full Hamiltonian into the reference and external interaction parts, this method adopts *ab initio* nuclear structure calculations for the eigenbases of the reference Hamiltonian. An importance truncation scheme is applied to trim the basis, where the Trotterized time-evolution operator is then applied to account for the time-dependent external interaction. By qubitizing the basis representation, the quantum circuit is prepared according to the time-evolution operator and is passed to the quantum computer for simulations. For this explanatory work, we illustrate this method by studying the Coulomb excitation of the deuteron, where the quantum simulations are performed with IBM Qiskit.

1 Introduction

Following Richard Feynman's original idea of simulating quantum dynamics using another well-controlled quantum system [1], the last couple of decades have witnessed the exciting innovation and rapid development of quantum computing technology. Quantum computers take advantage of quantum principles to potentially outperform their classical counterparts by increasing the computing power and reducing the required computing resources [2]. Widely celebrated algorithmic innovations such as the Shor's algorithm [3] and the quantum Fourier transformation [2, 4–6] fuel the excitement by proving the dramatic exponential speedup in computation compared to the classical computers. To exploit the power of the quantum computer, researchers have since developed various algorithms for Hamiltonian dynamics [7–12], with applications to problems in, e.g., condensed matter physics [13], quantum chemistry [14–17], nuclear physics [18, 19], and quantum field theories [20–23].

Here we present the hybrid quantum/classical algorithm for the time-dependent basis function on qubits (tBFQ) approach to nuclear inelastic scattering. It is a non-perturbative approach for quantum simulation

*duweigy@gmail.com

of the nuclear inelastic scattering processes. This is a quantum treatment of nuclear inelastic scattering that is adaptable for atomic and molecular quantum scattering as well. In this work, we will show 1) how to prepare and to qubitize the basis representation; 2) how to prepare the quantum algorithm for evolving the reaction system in a fully coherent manner on a quantum computer.

In particular, we adopt the interaction picture and divide the full Hamiltonian of the nuclear system undergoing inelastic scattering into the reference and external interaction parts. We first solve the eigenbasis set of the reference Hamiltonian via nuclear structure calculations on classical computers. Our eigenbasis is obtained from *ab initio* methods [24–28], but eigenbases from phenomenological models would also serve our purposes. We then apply an importance truncation scheme to regulate the basis size. With this trimmed basis set, we construct the basis representation in which we solve the time-dependent interaction Hamiltonian. Next, we qubitize the basis representation, which includes preparing the quantum circuit for the time-evolution for submission to the quantum computer. Finally, we evolve the inelastic scattering processes on the quantum computer. The measurements produce the transition probabilities as well as other observables of the reaction system.

The following features distinguish our work: 1) we solve the non-perturbative inelastic scattering process in the interaction picture, instead of the Schrödinger picture, which reduces complexity for quantum computation (see discussions in Sec. 2.1); 2) we adopt the basis representation prepared by a classical *ab initio* nuclear structure calculation, where both the bound and scattering states of the reference nuclear system are included; 3) we trim the dimension of the basis representation by an importance truncation scheme, which is an effective approach to control the dimension of the Hamiltonian for simulation while retaining the predominant reaction physics; 4) we map the basis representation to the qubit representation, with the potential for an exponential gain in computational power that is desirable for many-body applications (see, e.g., Ref. [17]).

In this work, we demonstrate the tBFQ algorithm with a simple model problem: the Coulomb excitation of the deuteron in the peripheral scattering with a heavy ion. This specific application served as a benchmark test in our previous works [29, 30] where we developed the time-dependent basis function (tBF) approach on classical computers to achieve a unified description of nuclear structure and reactions. This is a non-trivial problem due to the strong time-dependent external field that features higher-order transitions to states not directly accessible from the initial state. A generalization of this test application has successfully reproduced the experimental results [31]. Here, we similarly benchmark the tBFQ algorithm with this model problem applying the IBM Qiskit quantum simulator [32, 33].

The arrangement of this paper is as follows. In Sec. 2, we discuss the elements of the theory, including the Hamiltonian dynamics, our time-evolution scheme, and the construction of the basis representation. In this section, we also present the algorithm of the tBFQ. In Sec. 3, we present the details of the model problem. In Sec. 4, we illustrate the simulation conditions of the model problem and the corresponding results. We also compare the results of tBFQ with those of the tBF approach to validate the quantum simulation results.

We conclude with Sec. 5, where we provide an outlook.

2 Theory and Algorithm

2.1 Hamiltonian dynamics and time-evolution schemes

In the Schrödinger picture, the equation of motion of the reaction system is described by the time-dependent Schrödinger equation¹

$$i \frac{\partial}{\partial t} |\psi; t\rangle = H_{\text{full}}(t) |\psi; t\rangle. \quad (1)$$

The full Hamiltonian $H_{\text{full}}(t)$ can be divided into two self-adjoint terms:

$$H_{\text{full}}(t) = H_0 + V_{\text{int}}(t), \quad (2)$$

where H_0 denotes the the reference Hamiltonian (assumed to be time-independent) that determines the available excitations, while $V_{\text{int}}(t)$ is the external interaction that drives the dynamic excitation processes.

The state vector of the system at time $t \geq t_0$ can be solved as

$$|\psi; t\rangle = U(t; t_0) |\psi; t_0\rangle = \hat{T} \left\{ \exp \left[-i \int_{t_0}^t H_{\text{full}}(t') dt' \right] \right\} |\psi; t_0\rangle, \quad (3)$$

where $U(t; t_0)$ is the time-evolution operator that carries the system from t_0 to t . \hat{T} denotes the time-ordering operator towards the future and $|\psi; t_0\rangle$ the initial state vector of the system. Note that one would have $U(t; t_0) = \exp[-iH_{\text{full}}(t - t_0)]$ if H_{full} admits a simple time-independent form.

In practical quantum simulation of time-dependent $H_{\text{full}}(t)$, H_0 would result in additional computational complexities, i.e., more terms in the Trotterization procedures and more gates in the quantum circuit. Furthermore, we aim to be able to take advantage of advances in *ab initio* solutions of self-bound nuclei that also generate a discretized representation of states in the continuum. Hence, we choose to work in the interaction picture, where the equation of motion becomes:

$$i \frac{\partial}{\partial t} |\psi; t\rangle_I = V_{\text{int}}^I(t) |\psi; t\rangle_I, \quad (4)$$

with “ I ” denoting the interaction picture. $V_{\text{int}}^I(t)$ takes the form:

$$V_{\text{int}}^I(t) = e^{iH_0 t} V_{\text{int}}(t) e^{-iH_0 t}, \quad (5)$$

with $e^{\pm iH_0 t}$ resulting from the contribution of the reference Hamiltonian H_0 of the reaction system.

¹In this work, we adopt the natural units and take $\hbar = c = 1$.

Analogous to the formalism in the Schrödinger picture, the evolution of the state vector of the reaction system in the interaction picture $|\psi; t\rangle_I$ is

$$|\psi; t\rangle_I = U_I(t; t_0)|\psi; t_0\rangle_I = \hat{T} \left\{ \exp \left[-i \int_{t_0}^t V_{\text{int}}^I(t') dt' \right] \right\} |\psi; t_0\rangle_I, \quad (6)$$

where $U_I(t; t_0)$ denotes the unitary time-evolution operator. It evolves the state vector $|\psi; t_0\rangle_I$ at t_0 to any state vector $|\psi; t\rangle_I$ at $t \geq t_0$. In this work, we interrogate the inelastic scattering process by simulating $U_I(t; t_0)$.

2.2 Basis representation

For a full Hamiltonian of N_d degrees of freedom (or dimension of the Hamiltonian in a matrix representation), quantum computers take $\text{poly}(N_d, \delta t)$ number of gates to simulate the time-evolution operator for a given time increment δt . In order to achieve efficiency, it is important to select a basis representation that minimizes the essential degrees of freedom of the full Hamiltonian. While the lattice representation [21, 34] and the particle number representation (see, e.g., Refs. [17, 35]) could also work in reducing the dimension of the reaction problems, we suggest that the basis representation is advantageous because of its capacity to incorporate both the bound and scattering channels of nuclear systems.

The construction of a basis representation suitable for our test application has been detailed in our previous works [29–31]. In particular, we solve the eigenequation of the reference Hamiltonian H_0 [Eq. (2)] of the reaction system:

$$H_0|\beta_j\rangle = E_j|\beta_j\rangle, \quad (7)$$

where E_j denotes the eigenenergy corresponding to the eigenvector $|\beta_j\rangle$. The subscript “ j ” is an index which runs over individual state vectors. The eigenbasis set $\{|\beta_j\rangle\}$ is then applied to form the basis representation for the reaction system that will be subject to the external interaction. In principle, the basis set has infinite dimension so we apply an importance truncation scheme to regulate the basis size while retaining the predominant inelastic scattering physics (see, e.g., an example in Ref. [31], where we verified the independence of the obtained results from basis parameters and from the basis cutoff).

Within this finite basis representation, we evaluate the external interaction $V_{\text{int}}^I(t)$ [Eq. (5)] in the interaction picture as:

$$\langle\beta_i|V_{\text{int}}^I(t)|\beta_j\rangle = e^{i(E_i-E_j)t} \langle\beta_i|V_{\text{int}}(t)|\beta_j\rangle. \quad (8)$$

We remark that the contribution of the reference Hamiltonian H_0 is encoded in the phase factor $e^{i(E_i-E_j)t}$ for the interaction matrix element.

The state vector of the reaction system in the basis representation is

$$|\psi; t\rangle_I = \sum_j C_j^I(t) |\beta_j\rangle, \quad (9)$$

with the amplitude $C_j^I(t) \equiv \langle \beta_j | \psi; t \rangle_I$ corresponding to the basis $|\beta_j\rangle$. In general, the expectation value for the operator O representing an observable of the reaction system may be expressed using the fully entangled state of the reaction system as

$${}_I\langle \psi; t | O_I | \psi; t \rangle_I = \sum_{j,k} C_j^{I*}(t) C_k^I(t) \langle \beta_j | O_I | \beta_k \rangle. \quad (10)$$

However, an experiment corresponding to this operator makes a projection onto an available state in the basis space of the reaction system leading to a measurement of the expectation value $\langle O(t) \rangle$ according to the formalism of the ensemble average:

$$\langle O(t) \rangle = \sum_j p_j(t) \langle O_I \rangle_j, \quad (11)$$

where $p_j(t) \equiv |C_j^I(t)|^2$ and $\langle O_I \rangle_j \equiv \langle \beta_j | O_I | \beta_j \rangle$. In this work, we adopt Eq. (11) to evaluate observables of the reaction system.

The basis representation can be mapped to the qubit representation (known as qubitization) by relating each basis state to a unique qubit configuration (see in Sec. 4 for detailed illustrations). This mapping enables the evolution of N_d basis states (i.e., the degrees of freedom of the Hamiltonian) to be calculated with $\lceil \log_2 N_d \rceil$ qubits.

2.3 Algorithm

For our protocol of the nuclear inelastic scattering problem, we first prepare the initial state of the reaction system. We take the initial state of a quantum simulator to be the qubit configuration $|000\cdots\rangle \equiv |\uparrow\uparrow\uparrow\cdots\rangle$. Other versions of the initial state can be created by applying, e.g., the Pauli-X and/or the Hadamard gate(s), which provide the desired qubit configuration and/or entanglement [2]. After the initial state of the reaction system is properly prepared, we implement the time evolution for the system on the quantum computer, which proceeds with the steps outlined below.

First, we discretize the scattering duration into n equal time steps, with the step length $\delta t = (t - t_0)/n$. The time-evolution operator [Eq. (6)] can then be approximated as

$$U_I(t; t_0) \approx \hat{T} \left\{ \exp \left[-i [V_{\text{int}}^I(t) \delta t + V_{\text{int}}^I(t_{n-1}) \delta t + \cdots + V_{\text{int}}^I(t_1) \delta t] \right] \right\}. \quad (12)$$

The accuracy of this approximation depends on the magnitude of δt . In principle, we require $\|V_{\text{int}}^I(t_i)\| \cdot \delta t \ll 1$

for any moment $t_i \in [t_0, t]$.

Next, we approximate $U_I(t; t_0)$ into a series of unitary evolution operations according to the first-order Trotterization [2]:

$$U_I(t; t_0) = \underbrace{e^{-iV_{\text{int}}^I(t)\delta t}}_{U(t; t_{n-1})} \dots \underbrace{e^{-iV_{\text{int}}^I(t_k)\delta t}}_{U(t_k; t_{k-1})} \dots \underbrace{e^{-iV_{\text{int}}^I(t_1)\delta t}}_{U(t_1; t_0)} + \mathcal{O}(\delta t^2). \quad (13)$$

The accuracy of the first-order Trotterization is up to $(\delta t)^2$ [2]. Note that we can improve our approximation of $U_I(t; t_0)$ by applying higher-order Trotterization formalism [36, 37].

Then, we prepare the quantum circuit according to the sequence of Trotterization steps in Eq. (13). Since our goal here is to present the methodology to simulate nuclear inelastic scattering processes on quantum computers, we show a simple and direct approach to construct the circuit. To improve the circuit by, e.g., reducing the number of CNOT gates and the circuit length, is beyond the scope of this paper and will be deferred to future works. Our prescription of the circuit preparation is as follows:

1. We first evaluate each Trotterization step $U(t_k; t_{k-1})$ in the basis representation constructed by the set $\{|\beta_j\rangle\}$ (recall the construction of the basis representation discussed in Sec. 2.2).
 - (a) We start with solving the eigenvalue problem of the external interaction $V_{\text{int}}^I(t_k)$:

$$V_{\text{int}}^I(t_k)|\xi_{k\alpha}\rangle = v_{k\alpha}|\xi_{k\alpha}\rangle, \quad (14)$$

where $v_{k\alpha}$ is the eigenvalue corresponding to the eigenvector $|\xi_{k\alpha}\rangle$. The subscript k denotes the k^{th} Trotterization step, while α labels the eigenvectors of $V_{\text{int}}^I(t_k)$. We remark that, for each eigenvector $|\xi_{k\alpha}\rangle$, the following identity holds [38]:

$$\exp[-iV_{\text{int}}^I(t_k)\delta t]|\xi_{k\alpha}\rangle = \exp[-iv_{k\alpha}\delta t]|\xi_{k\alpha}\rangle. \quad (15)$$

We work in the basis representation, where the matrix elements of $V_{\text{int}}^I(t_k)$ are evaluated according to Eq. (8), while each eigenvector $|\xi_{k\alpha}\rangle$ admits the following form:

$$|\xi_{k\alpha}\rangle = \sum_j a_{k\alpha j} |\beta_j\rangle, \quad (16)$$

with the amplitude $a_{k\alpha j} \equiv \langle \beta_j | \xi_{k\alpha} \rangle$.

- (b) Therefore, in the basis representation, $U(t_k; t_{k-1})$ can then be written as

$$U(t_k; t_{k-1}) = UU_d U^\dagger, \quad (17)$$

where the transformation matrix U is formed from the amplitudes $\{\langle \beta_j | \xi_{k\alpha} \rangle\}$, while U_d is the

diagonal matrix with elements $\{e^{-iv_{k\alpha}\delta t}\}$.

2. We then qubitize the basis representation. During the qubitization, each unitary $U(t_k; t_{k-1})$ is decomposed into the standard CNOT and single-qubit gates [2]. This can be done with schemes such as the quantum Shannon decomposition, the cosine-sine decomposition or the column-by-column decomposition (see Ref. [39] and references therein). In practice, we approach the decomposition by the quantum Shannon decomposition scheme applying the UniversalQCompiler package [40].
3. We combine the sequence of gates decomposed from all the unitaries in Eq. (13) to create the complete quantum circuit, which is passed to the quantum computer for simulating the nuclear inelastic scattering. The total number of the gates is expected to be polynomial in the $\lceil \log_2 N_d \rceil$ (N_d here being the dimension of the basis representation) and the scattering duration $(t - t_0)$.

In each quantum simulation, we evolve the quantum circuit to a fixed time t during the inelastic scattering, at which point we measure all the qubits simultaneously and therefore collapse the wave function of the reaction system. After a set of such simulations, we collect the probabilities of basis states $\{|C_j^I(t)|^2\}$, which represent our knowledge of the reaction system. According to the probabilities $\{|C_j^I(t)|^2\}$, the observables of the reaction system can then be computed by taking the ensemble average [Eq. (11)].

3 Model problem

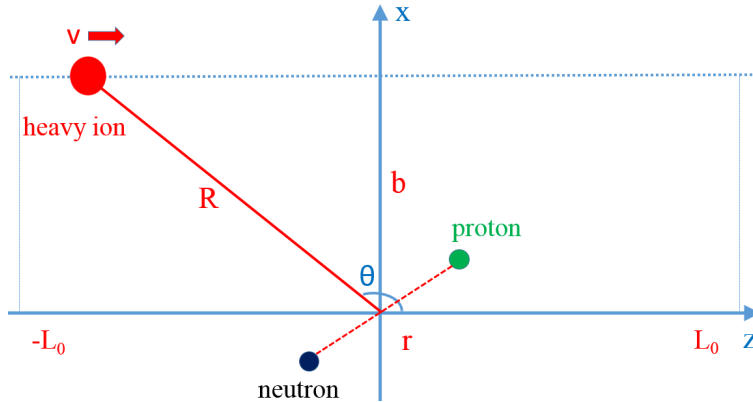


Figure 1: (Color online) Setup for the Coulomb excitation of the deuteron in the peripheral collision with a heavy ion (adopted from Refs. [29,30]). See the text for more details.

We demonstrate this algorithm by applying it to a model problem: the Coulomb excitation of the deuteron in a peripheral collision with a heavy ion. In our previous papers, we introduced the time-dependent basis function (tBF) method and solved this test problem on classical computers [29,30]. Here, we only describe some of the necessary details to make our discussion self-contained.

Our setup of the model problem is shown in Fig. 1. We work in the center-of-mass frame of the deuteron target and take the scattering plane to be the xz plane. For the purpose of illustration, we place the deuteron

target in a weak harmonic oscillator trap. This trap regulates the continuum states and localizes the center-of-mass motion of the deuteron to simplify the problem. We assume that the neutron and proton are both point-like and the proton carries the unit charge $+e$. \vec{r} denotes the position vector of the proton with respect to the neutron. The separation between the nucleons is then $r \equiv |\vec{r}|$. The projectile is a heavy ion, which carries charge Ze and travels with a constant velocity \vec{v} parallel to the \hat{z} axis. \vec{R} denotes the position vector of the heavy ion from the origin. The impact parameter is b .

In this demonstration problem, we will neglect nuclear interactions between the target and the projectile and focus only on the deuteron target scattered by the external electromagnetic field produced by the heavy ion. Following our analyses in Refs. [29, 30], the total time-dependent Hamiltonian of the target is given by Eq. (2), where H_0 is taken as the reference Hamiltonian that describes the intrinsic motion of the target:

$$H_0 = T_{\text{rel}} + V_{\text{NN}} + U_{\text{trap}}, \quad (18)$$

with T_{rel} being the relative kinetic energy of the neutron and the proton and V_{NN} the nucleon-nucleon interaction. U_{trap} denotes the external harmonic oscillator trap acting on the intrinsic degree of freedom of the target.

As explained in Sec. 2.2, we employ H_0 to solve for the eigenbasis set of the target $\{|\beta_j\rangle\}$. While the deuteron can be solved easily by numerous techniques, we adopt the techniques of the No-Core Shell Model [24–27] anticipating the applications of this formalism for larger systems of nucleons. We neglect the excitations of the center of mass of the two-body system in this model application and focus on its internal excitations. In more realistic applications, the center of mass motion is not constrained by a trap and there is no effect of a trap on the intrinsic motion [31].

At the limit of low incident speed $|\vec{v}|$, the external interaction $V_{\text{int}}(t)$ can be approximated by the major contribution from the electric dipole ($E1$) component of the time-varying Coulomb field [41, 42]. In the basis representation, the external interaction in the interaction picture reads:

$$\langle\beta_j|V_{\text{int}}^I(t)|\beta_k\rangle = \frac{4\pi}{3}Ze^2e^{i(E_j-E_k)t}\sum_{\mu}\frac{Y_{1\mu}^*(\Omega_R)}{|R(t)|^2}\int d\vec{r}\langle\beta_j|\vec{r}\rangle\frac{r}{2}Y_{1\mu}(\Omega_r)\langle\vec{r}|\beta_k\rangle, \quad (19)$$

where $Y_{\lambda\mu}$ denotes the spherical harmonics [43]: $\lambda = 1$ denotes the $E1$ component of the Coulomb field. The solid angles Ω_R and Ω_r are specified by the polar and azimuth angles of \vec{R} and \vec{r} , respectively. The unitary time-evolution operator for each Trotterization step in Eq. (13) can be evaluated based on Eq. (19).

4 Simulation conditions and results

We take the projectile to be a fully stripped uranium nucleus, U^{92+} , which is treated as a point-like source of the time-varying external Coulomb potential. The incident speed is set to be 0.1 in units of the speed of light, while the impact parameter is chosen to be 5 fm. We also take the exposure time to be from -3 to 3 MeV $^{-1}$,

Table 1: Selected basis states of the deuteron target in the model problem. The target is confined in an external harmonic oscillator trap of strength 5 MeV and the center-of-mass motion of the target is restricted to the lowest state of the trap. The first and second columns present the quantum numbers of the selected states. The third and fourth columns present, respectively, the eigenenergy and the *r.m.s.* point-charge radius of each state: they contribute to the intrinsic energy and *r.m.s.* point-charge radius of the target according to Eq. (11). The last column shows the 3-qubit configurations corresponding to these selected states.

Channel	Magnetic substate	$\langle E \rangle$ [MeV]	$\langle r^2 \rangle^{\frac{1}{2}}$ [fm]	Qubit configuration
$(^3S_1, ^3D_1)$	$M = -1$	-0.65289	1.47222	$ 000\rangle$
	$M = 0$			$ 100\rangle$
	$M = +1$			$ 010\rangle$
3P_0	$M = 0$	12.0733	3.13427	$ 110\rangle$
3P_1	$M = -1$	12.7585	3.27644	$ 001\rangle$
	$M = 0$			$ 101\rangle$
	$M = +1$			$ 011\rangle$

which corresponds to a time duration of approximately 4.0×10^{-21} sec. That is, the time evolution starts when the uranium is about 60 fm before its closest approach to the origin, and concludes when the uranium is in the position 60 fm after the closest approach. Beyond this region, the induced intrinsic excitations of the target are negligible since the Coulomb field is sufficiently weak compared with the available excitations.

We choose the same basis representation as in our previous works Refs. [29,30]. In particular, we obtain the basis states (or reaction channels) of the target $\{|\beta_j\rangle\}$ according to Eq. (7). For this demonstration, we trim the basis size and retain only the lowest seven states in three interaction channels: $(^3S_1, ^3D_1)$, 3P_0 , and 3P_1 . These states are listed in Table 1, based on which we construct the basis representation for our model problem. Our basis representation can be directly mapped to a 3-qubit representation, as provided in the last column in Table 1.

We simulate our model problem on an ideal quantum simulator provided by IBM Qiskit [32,33]. The initial state of the target in our simulations are chosen to be $(^3S_1, ^3D_1), M = -1$, which corresponds to the $|000\rangle$ state. In our simulation, we take the Trotterization time step $\delta t = 0.01$ MeV $^{-1}$. In principle, a finer time-step improves the accuracy in the Trotterization [Eq. (13)] at the cost of circuit complexity [2].

The transition probabilities of all the retained channels (Table 1) are presented in panels (a)-(g) of Fig. 2. For comparison, we also show the results computed by the non-perturbative method based on a classical algorithm, the time-dependent basis function (tBF) [29]. We find good agreement between the results calculated by the quantum and classical algorithms.²

We work with the ideal quantum simulator. Besides the error from the approximation of the first-order Trotterization, which is at the order of $(\delta t)^2$, there is the expected variance from quantum mechanical measurement, which is statistical. For the current work, we take 10 quantum simulations (each with 10^7

² As a crosscheck, we also calculate the “Trotterized” evolution via the classical approach. This is achieved by sequentially multiplying matrices of dimension $2^3 \times 2^3$ according to Eq. (13). We find that the classical Trotterization results agree well with the tBF results (within the error of less than 1% for each state). Since in panels (a)-(g) of Fig. 2, the curves of the tBF and the classical Trotterization results overlap with each other, we do not present explicitly the classical Trotterization results.

measurements) for every chosen evolution time shown in Fig. 2. The resulting statistical errors are less than 1% for most of the retained states, except for $^3P_0, M=0$ and $^3P_1, M=0$, where such errors are less than 4%. We remark that these statistical errors are expected to decrease with increasing number of simulations. In Fig. 2, we do not show the error bars explicitly since they are smaller than the size of the symbols in the plots.

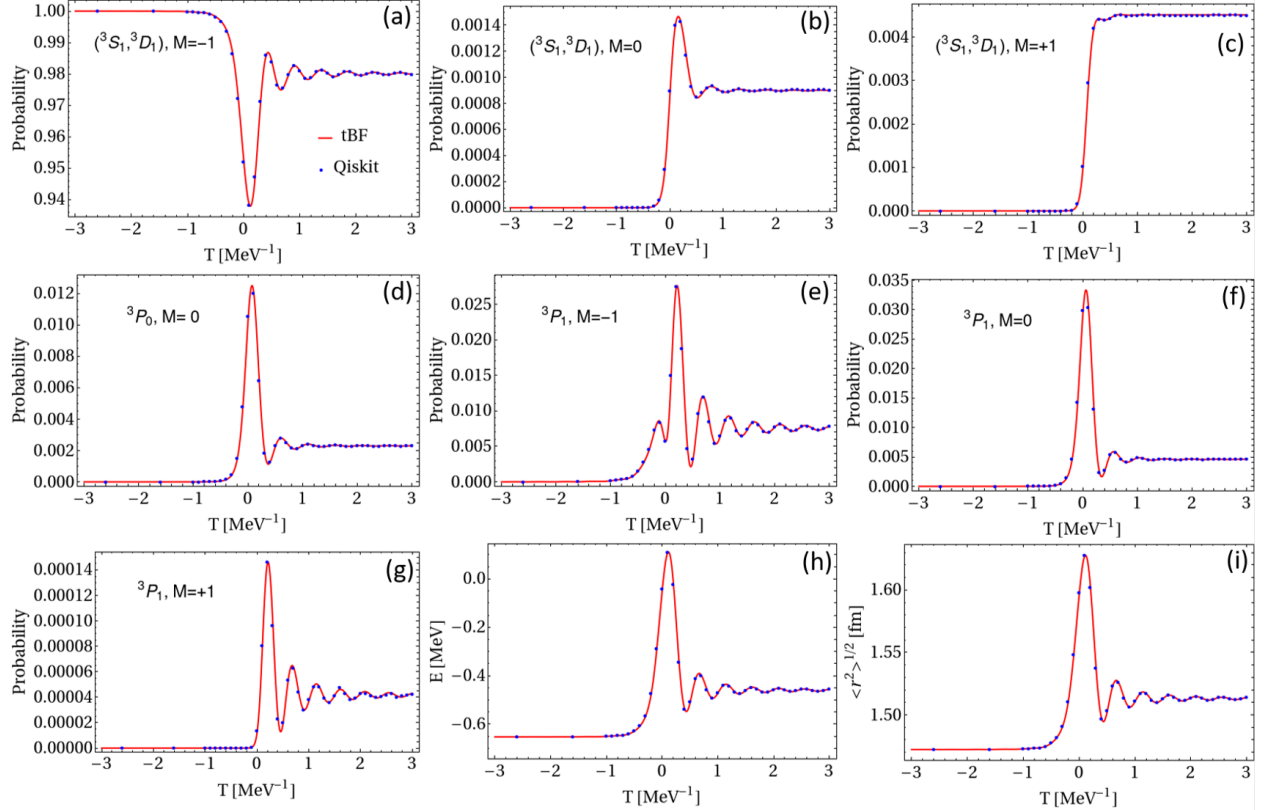


Figure 2: (Color online) Transition probabilities and scattering observables calculated by the tBF method and the tBFQ method. Panels (a)-(g) [panel (a) presenting the initial state] are the transition probabilities of the selected basis states in Table 1. Panels (h) and (i) show the excitation of intrinsic energy and the expansion of the state-average *r.m.s.* point-charge radius of the deuteron system arising from the Coulomb excitation, where the results are obtained by both the classical tBF method (smooth red lines in each panel) and the tBFQ method via quantum simulations on IBM Qiskit (discrete blue points in each panel).

In Fig. 2, we also present the results of the two selected observables, i.e., the intrinsic energy [panel (h)] and the state-average *r.m.s.* point-charge radius of the deuteron target [panel (i)] throughout the Coulomb excitation process.³ These observables can be obtained according to Eq. (11). As may be expected from the good agreement in the state population obtained from the quantum and the classical methods, the corresponding results of the observables also show a good agreement. Working with the ideal quantum computer simulator, we note that the error bars of the results from the quantum simulations come mainly from the statistics in quantum measurement. These error bars are smaller than the size of the symbols and

³We remark that the state-average *r.m.s.* point-charge radius of the deuteron target is measured with respect to the center-of-mass so this radius is 1/2 of the separation *r* defined above.

are hence omitted.

Finally, we remark that the quantum evolution according to the tBFQ algorithm is fully coherent. That is, the wave function of the deuteron evolves in a fully coherent way during the simulation until it collapses in measurement. This is one of the appealing aspects of Feynman’s original idea [1] of simulating one quantum system via another one, in which the full coherence (and also entanglement) is preserved naturally. In addition, tBFQ is a non-perturbative approach. By keeping only the dominant $E1$ multipole component of the Coulomb field, one would expect populations in the states $^3P_0, M = 0$; $^3P_1, M = -1$; and $^3P_1, M = 0$, according to the $E1$ selection rule [recall that we prepare the initial state to be $(^3S_1, ^3D_1), M = -1$]. However, tBFQ keeps all the higher-order effects (e.g., sequential $E1$ excitations) as well, which contribute to a complicated transition network among these seven retained states. As a result, this network feeds the $E1$ forbidden states that can not be directly populated from the initial state, such as $(^3S_1, ^3D_1), M = +1$, during the Coulomb excitation.

5 Conclusion and Outlook

We present the algorithm for the time-dependent basis function treatment of nuclear inelastic scattering on qubits (tBFQ). This *ab initio*, non-perturbative algorithm provides a hybrid quantum/classical approach for simulating nuclear inelastic scattering problems.

For tBFQ, we work in the interaction picture in which we divide the full Hamiltonian of the nuclear system undergoing inelastic scattering into the reference Hamiltonian (presumably time-independent), which determines the available excitations of that system, and the external interaction, which drives the dynamical excitation processes. We solve for the eigenbases of the reference Hamiltonian and apply an importance truncation to reduce the basis set. This trimmed basis set is used to construct the basis representation, within which we solve the external interaction and hence the time-evolution operator by Trotterization. The basis representation is then mapped to the qubit representation. In this qubitization process, the quantum circuit is prepared according to the time-evolution operator and is passed to the quantum computer for simulations. According to the measurements of the simulation, we obtain the transition probabilities (which in turn determine the inelastic scattering cross section) and the other observables of the reaction system.

For illustrative purposes, we demonstrate this algorithm with a model problem, Coulomb excitation of the deuteron in a peripheral collision with a heavy ion. The results of the transition probabilities and the selected observables computed by the tBFQ algorithm applying the IBM Qiskit quantum simulator agree well with the corresponding results computed by classical methods.

The promise of quantum computers is that the computational complexity of many-body Hamiltonian dynamics can be exponentially reduced. However, many challenges exist. Going forward, the optimization of the algorithm, e.g., constructing efficient quantum circuits [44, 45], will be necessary for simulations of general reaction problems on real quantum computers. The general features of our algorithm allow its use

for studying many-body Hamiltonian dynamics in atomic and subatomic physics.

Acknowledgments

This work was supported in part by the US Department of Energy (DOE) under Grants No. DE-FG02-87ER40371, No. DE-SC0018223 (SciDAC-4/NUCLEI), and No. DESC0015376 (DOE Topical Collaboration in Nuclear Theory for Double-Beta Decay and Fundamental Symmetries). A portion of the computational resources were provided by the National Energy Research Scientific Computing Center (NERSC), which is supported by the US DOE Office of Science. X.Z. and W.Z. are supported by the Strategic Priority Research Program of Chinese Academy of Sciences, Grant No. XDB34000000. X.Z. is supported by new faculty startup funding from the Institute of Modern Physics, Chinese Academy of Sciences and by Key Research Program of Frontier Sciences, CAS, Grant No. ZDBS-LY-7020. W.Z. are supported by the National Natural Science Foundation of China (Grants No. 11975282 and No. 11435014) and the 973 Program of China (Grant No. 2013CB834405). We acknowledge P. Yin and Y. Li for their valuable input. W.D. and J.P.V. thank H. Lamm, G. R. Luecke, R. Basili and D. Zhao for valuable discussions.

References

- [1] R. P. Feynman, *Int. J. Theor. Phys.* **21**, 467 (1982). doi:10.1007/BF02650179
- [2] M. A. Nielsen and I. L. Chuang, *Quantum computation and quantum information* (Cambridge University Press, Cambridge, 2000).
- [3] P. W. Shor, *SIAM Journal on Computing*, 26(5):1484-1509, 1997. [arXiv:quant-ph/9508027](#).
- [4] D. Coppersmith, *An approximate Fourier transform useful in quantum factoring*, IBM Research Report RC 19642 (1994).
- [5] A. Ekert and R. Jozsa, *Rev. Mod. Phys.* **68**, 733 (1996).
- [6] D. Camps, R. V. Beeumen, C. Yang, *arXiv*: 2003.03011 [math.NA].
- [7] S. Lloyd, *Science* **273**, 1073 (1996).
- [8] A. M. Childs, Ph.D. thesis, Massachusetts Institute of Technology, 2004.
- [9] D. W. Berry, G. Ahokas, R. Cleve, and B. C. Sanders, *Commun. Math. Phys.* **270**, 359 (2007).
- [10] A. M. Childs and R. Kothari, *Theory of Quantum Computation, Communication, and Cryptography*, Lecture Notes in Computer Science, Vol. 6519 (Springer, Berlin, 2011), p. 94.
- [11] D. Poulin, A. Qarry, R. D. Somma, and F. Verstraete, *Phys. Rev. Lett.* **106**, 170501 (2011).

- [12] D. W. Berry and A. M. Childs, Quantum Inf. Comput. **12**, 29 (2012).
- [13] A. Macridin, P. Spentzouris, J. Amundson, R. Harnik, Phys. Rev. Lett. **121**, 110504 (2018).
- [14] B. P. Lanyon, J. D. Whitfield, G. G. Gillett, M. E. Goggin, M. P. Almeida, I. Kassal, J. D. Biamonte, M. Mohseni, B. J. Powell, M. Barbieri, et al., Nature chemistry **2**, 106 (2010).
- [15] J. I. Colless, V. V. Ramasesh, D. Dahlen, M. S. Blok, M. E. Kimchi-Schwartz, J. R. McClean, J. Carter, W. A de Jong, and I. Siddiqi, Phys. Rev. X **8**, 011021 (2018).
- [16] R. Babbush, J. McClean, D. Wecker, A. Aspuru-Guzik, N. Wiebe, Phys. Rev. A **91**, 022311 (2015).
- [17] S. McArdle, S. Endo, A. Aspuru-Guzik, S. Benjamin, X. Yuan, Rev. Mod. Phys. **92**, 15003 (2020).
- [18] E. F. Dumitrescu *et al.*, Phys. Rev. Lett. **120**, no. 21, 210501 (2018) doi:10.1103/PhysRevLett.120.210501 [[arXiv:1801.03897](#) [quant-ph]].
- [19] A. Roggero and J. Carlson, Phys. Rev. C **100**, no. 3, 034610 (2019) doi:10.1103/PhysRevC.100.034610 [[arXiv:1804.01505](#) [quant-ph]].
- [20] N. Klco *et al.*, Phys. Rev. A **98**, no. 3, 032331 (2018) doi:10.1103/PhysRevA.98.032331 [[arXiv:1803.03326](#) [quant-ph]].
- [21] N. Klco and M. J. Savage, Phys. Rev. A **99**, no. 5, 052335 (2019) doi:10.1103/PhysRevA.99.052335 [[arXiv:1808.10378](#) [quant-ph]].
- [22] A. Alexandru *et al.* [NuQS Collaboration], Phys. Rev. Lett. **123**, no. 9, 090501 (2019) doi:10.1103/PhysRevLett.123.090501 [[arXiv:1903.06577](#) [hep-lat]].
- [23] H. Lamm *et al.* [NuQS Collaboration], Phys. Rev. D **100**, no. 3, 034518 (2019) doi:10.1103/PhysRevD.100.034518 [[arXiv:1903.08807](#) [hep-lat]].
- [24] B. R. Barrett, P. Navratil and J. P. Vary, Prog. Part. Nucl. Phys. **69**, 131 (2013). doi:10.1016/j.ppnp.2012.10.003
- [25] P. Navratil, V. G. Gueorguiev, J. P. Vary, W. E. Ormand and A. Nogga, Phys. Rev. Lett. **99**, 042501 (2007) doi:10.1103/PhysRevLett.99.042501 [[nucl-th/0701038](#)].
- [26] P. Navratil, J. P. Vary and B. R. Barrett, Phys. Rev. Lett. **84**, 5728 (2000) doi:10.1103/PhysRevLett.84.5728 [[nucl-th/0004058](#)].
- [27] P. Navratil, J. P. Vary and B. R. Barrett, Phys. Rev. C **62**, 054311 (2000). doi:10.1103/PhysRevC.62.054311
- [28] J. Carlson, S. Gandolfi, F. Pederiva, S. C. Pieper, R. Schiavilla, K. E. Schmidt and R. B. Wiringa, Rev. Mod. Phys. **87**, 1067 (2015) doi:10.1103/RevModPhys.87.1067 [[arXiv:1412.3081](#) [nucl-th]].

- [29] W. Du, P. Yin, Y. Li, G. Chen, W. Zuo, X. Zhao and J. P. Vary, Phys. Rev. C **97**, no. 6, 064620 (2018) doi:10.1103/PhysRevC.97.064620 [[arXiv:1804.01156](#) [nucl-th]].
- [30] W. Du, P. Yin, G. Chen, X. Zhao and J. P. Vary, [arXiv:1704.05520](#) [nucl-th].
- [31] P. Yin, W. Du, W. Zuo, X. Zhao and J. P. Vary, [arXiv:1910.10586](#) [nucl-th].
- [32] Alan C. Santos, Rev. Bras. Ens. Fis. 39(1), e1301 (2017). [arXiv:1610.06980](#) [quant-ph].
- [33] A. W. Cross, L. S. Bishop, J. A. Smolin, and J. M. Gambetta, arXiv preprint [arXiv:1707.03429](#) (2017).
- [34] J. B. Kogut, Rev. Mod. Phys. **51**, 659 (1979). doi:10.1103/RevModPhys.51.659
- [35] G. Ortiz, J.E. Gubernatis, E. Knill, R. Laflamme, Phys. Rev. A **64**, 022319 (2002).
- [36] N. Hatano, M. Suzuki, *Finding exponential product formulas of higher orders*, in Lect. Notes Phys. **679**, 37–68 (2005).
- [37] A. Smith, M. S. Kim, F. Pollmann, J. Knolle, npj Quantum Information **5**, 106 (2019). [arXiv:1906.06343](#) [quant-ph].
- [38] G. B. Arfken, H. J. Weber, F. E. Harris, *Mathematical Methods for Physicists: A Comprehensive Guide*, 7th ed (Academic Press, US, 2011).
- [39] R. Iten, R. Colbeck, I. Kukuljan, J. Home, and M. Christandl Phys. Rev. A **93**, 032318.
- [40] R. Iten, O. R. Smith, L. Mondada, E. Redmond, R. S. Kohli, R. Colbeck, [arXiv:1904.01072](#).
- [41] A. Bohr and B. Mottelson, *Nuclear Structure, Vol. 1* (World Scientific, Singapore, 1998), p. 92.
- [42] K. Alder, A. Bohr, T. Huus, B. Mottelson and A. Winther, Rev. Mod. Phys. **28**, 432 (1956). doi:10.1103/RevModPhys.28.432
- [43] J. Suhonen, *From Nucleons to Nucleus: Concepts of Microscopic Nuclear Theory* (Springer-Verlag, Berlin, 2007).
- [44] D. W. Berry, A. M. Childs, R. Cleve, R. Kothari, and R. D. Somma Phys. Rev. Lett. **114**, 090502 (2015)
- [45] D. W. Berry, A. M. Childs, R. Cleve, R. Kothari, and R. D. Somma, in *Proceedings of the 46th Annual ACM Symposium on Theory of Computing, New York, 2014* (ACM Press, New York, 2014), pp. 283-292.